

An Original Approach to Determine the Minimum Operating Frequency of Mode-Stirred Reverberation Chambers

Lionel Michard^{1,*}, Guillaume Andrieu¹, Philippe Leveque¹, and Delia Arnaud-Cormos^{1,2}

¹University of Limoges, XLIM, CNRS, UMR 7252, Limoges, France

²Institut Universitaire de France (IUF), Paris, France

ABSTRACT: The minimum operating frequency (MOF) of mode-stirred reverberation chambers is often assessed through statistical analysis using goodness-of-fit (GoF) statistical hypothesis tests such as Anderson-Darling or Kolmogorov-Smirnov. However, in the context of MOF determination, hypothesis tests are typically used with the aim of proving the null hypothesis made on the probability distribution of the electric field in the cavity, as opposed to the initial intent of the tests. A new approach avoiding hypothesis testing is proposed in this work by introducing a criterion based on normalized statistical distances. By normalizing the distances, it has been made possible to limit the influence of the sample size on the assessed minimum frequency, thereby improving the consistency of the results.

1. INTRODUCTION

Mode-stirred reverberation chambers (MSRCs) are widely used in many industries and research fields such as electromagnetic compatibility [1], bioelectromagnetics [2], and the food industry [3].

When employing or designing an MSRC, it is necessary to assess its operational frequency range. In order to consider an MSRC as overmoded, i.e., providing a sufficiently homogeneous and isotropic electric field [4], one may define a frequency corresponding to a sufficiently large number of overlapping modes. In this work, this frequency is referred to as the minimum operating frequency (MOF). The MOF can be assessed through different techniques, including statistical analysis. In the literature, statistical approaches often involve using goodness-of-fit (GoF) hypothesis tests such as Anderson-Darling (AD) [2, 5–8] or Kolmogorov-Smirnov (KS) [7, 9–11]. However, these tests are usually utilized in a way that consists of proving the null hypothesis, as opposed to their original purpose. It is shown in this work that this inversion adds uncertainty to the MOF determination.

GoF tests, such as AD and KS tests, use statistical distance concepts [12]. Within the context of this study, the term ‘statistical distance’ refers to the similarity between statistical distributions. The distances are used to compare the measured experimental distributions from the MSRC with the theoretical ones. Several different distances have been formulated by statisticians in the literature. To address this formulation diversity, a distance normalization procedure is proposed in this work.

This paper aims to discuss the use of hypothesis tests in the context of MOF assessment and proposes a statistical approach based on normalized statistical distances not relying on hypothesis testing.

* Corresponding author: Lionel Michard (lionel.michard@unilim.fr).

2. MODE-STIRRED REVERBERATION CHAMBER STATISTICS

2.1. Electric Field Probability Distribution

According to the literature, the rectangular (cartesian) components of the electric field in a perfectly overmoded MSRC are asymptotically Rayleigh distributed [4, 7, 10, 13]. The cumulative distribution function (CDF) of the Rayleigh distribution is given by:

$$F(x) = 1 - \exp\left(-\frac{x^2}{2\sigma^2}\right) \quad (1)$$

The Rayleigh distribution parameter σ can be estimated from a sample of size N by applying the maximum likelihood method. The resulting estimated parameter denoted as $\hat{\sigma}$ is given by:

$$\hat{\sigma} = \sqrt{\frac{1}{2N} \sum_{k=1}^N x_k^2} \quad (2)$$

One of the approaches to assess the MOF consists of analyzing the S parameters of the antenna(s) located in the chamber. For example, in the case of a linearly polarized antenna in a perfectly overmoded RC, the statistics of the magnitude of the reflection coefficient due to the stirred paths, $|S_{11}^{\text{sti}}|$, are considered to be the same as the statistics of the magnitude of the rectangular components of the electric field [5, 14–16].

The fact that the rectangular electric field magnitude is Rayleigh distributed implies that the MSRC is *overmoded*, also denoted as *well-stirred*. It has been shown that the electromagnetic properties inside a well-stirred MSRC are expected to be homogenous, at an electrically large distance away from the walls and objects [17]. Hence, it will be considered in this work that the whole working volume is well stirred as long as

TABLE 1. (a) Analytical and (b) equivalent computational formulae of the statistical distances used in this study.

(a)	
Distance Name	D_s
Anderson-Darling (AD) [19]	$N \int_{-\infty}^{+\infty} \frac{(F_n(x) - F(x))^2}{F(x)(1-F(x))} dF(x)$
Kolmogorov-Smirnov (KS) [19]	$\max_{x \in \mathbb{R}} F_n(x) - F(x) $
Cramer-von Mises (CvM) [19]	$N \int_{-\infty}^{+\infty} (F_n(x) - F(x))^2 dF(x)$
First-Order Wasserstein (FOW) [20]	$\int_{-\infty}^{+\infty} F_n(x) - F(x) dx$

(b)	
Distance Name	D_s
Anderson-Darling (AD) [5]	$-N - \sum_{k=1}^N \frac{2k-1}{N} [\ln(F(x_k)) + \ln(F(x_{N+1-k}))]$
Kolmogorov-Smirnov (KS) [19]	$\max_{k \in \llbracket 1; N \rrbracket} F_n(x_k) - F(x_k) $
Cramer-von Mises (CvM) [19]	$\frac{1}{12N} + \sum_{k=1}^N \left[\frac{2k-1}{2N} - F(x_k) \right]^2$
First-Order Wasserstein (FOW)	<i>Numerical integration of the analytical formula</i>

the $|S_{11}^{\text{sti}}|$ population is Rayleigh distributed. In other words, the measurements are performed at a single location in the MSRC and are considered sufficient to assess the homogeneity and isotropy in the whole working volume. More details on this inductive reasoning can be found in [5, 14].

To assess whether the $|S_{11}^{\text{sti}}|$ samples are Rayleigh distributed, goodness-of-fit (GoF) statistical hypothesis tests such as Kolmogorov-Smirnov (KS) or Anderson-Darling (AD) are often employed in the literature [2, 5–10, 18].

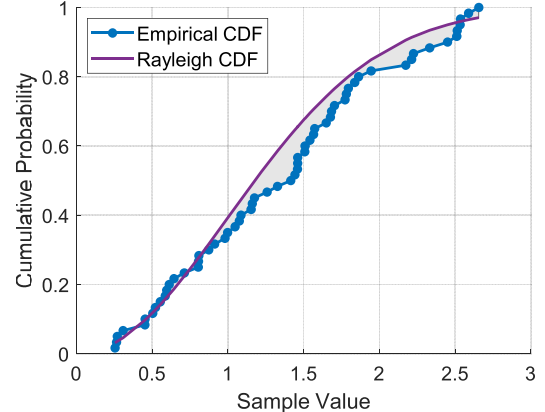
2.2. Statistical Hypothesis Tests

Statistical hypothesis tests assess the probability of observing some results in the conditions of the null hypothesis. This probability is often referred to as the statistical significance. Goodness-of-fit (GoF) tests are a type of hypothesis tests used to study the significance of a statistical sample by comparing its characteristics to a statistical model or to another sample. Comparison methods often consist of measuring the discrepancy between the empirical cumulative distribution function (ECDF) of the sample and the theoretical cumulative distribution function (CDF) associated with the hypothesized population probability distribution. Let (X_1, \dots, X_N) be a set of N independent observations. The ECDF denoted as $F_n(x)$ is the proportion of observations which are less or equal to x :

$$F_n(x) = \frac{|X_i \leq x|}{N} \quad (3)$$

where $|X_i \leq x|$ denotes the number of sample elements lower than x .

Figure 1 shows the ECDF of an example set of 50 observations of a Rayleigh distributed random variable. The shaded area between the curves is an image of the statistical distance between the ECDF and the theoretical CDF, i.e., the model dis-

**FIGURE 1.** Typical plots of ECDF ($N = 50$) and Rayleigh CDF.

crepancy. This distance can be probed using different formulae such as those listed in Table 1.

In this table, four different statistical distances denoted as D_s are given in their analytical form: Anderson-Darling (AD) [19], Kolmogorov-Smirnov (KS) [19], Cramer-von Mises (CvM) [19], and first-order Wasserstein (FOW) [20]. In every D_s formula, F_n refers to the empirical cumulative distribution function of the sample (ECDF) whereas F refers to the model cumulative distribution function, i.e., the Rayleigh CDF in the context of this work. For example, the KS distance measures the maximum distance between the ECDF and the CDF across all the sample values whereas the first-order Wasserstein distance measures the shaded area through Riemann integration. For more efficient computations, the computational forms of the statistical distances given in Table 1(b) are used in this study.

For GoF hypothesis tests, the null hypothesis H_0 and alternative hypothesis H_a can be formulated as follows:

H_0 : the observed sample is originating from the hypothesized distribution,
 H_a : the observed sample is not originating from the hypothesized distribution.

GoF tests use the statistical distance concept (denoted in this work as D_S) between the sample ECDF and hypothesized distribution CDF. The calculated D_S is compared to a threshold value t_α associated with a significance level α . The significance level is the probability to make a type I error, i.e., H_a is accepted whereas H_0 is actually true. Hence, when comparing the value of D_S to t_α , the possible outcomes are [21]:

$D_S \geq t_\alpha$ the result is considered as significant, and the alternative hypothesis H_a is accepted whereas the null hypothesis H_0 is rejected with a probability α to make a type I error,

$D_S < t_\alpha$ the result is considered as insignificant; H_a is not accepted; and one fails to reject H_0 .

Failing to reject H_0 does not mean that H_0 should be accepted either. As any other hypothesis tests, the AD and KS tests cannot prove the null hypothesis true. Indeed, these tests are rather designed to detect statistical anomalies, i.e., significant results [21]. Nevertheless, hypothesis tests are commonly used in the electromagnetic literature with the aim of proving the null hypothesis [2, 5–10, 18]. These findings motivated the proposal of the method presented in Section 5 which does not rely on hypothesis testing.

3. EXPERIMENTAL SETUP

To illustrate the concepts used in this paper, experimental data was generated using the setup shown in Figure 2. This setup is mainly composed of three components similar to [2]: a custom wideband patch antenna, an MSRC based on a biological incubator (BINDER CB 150 Gmbh, Tullingen, Germany), and a Vector Network Analyzer (8753E, Agilent, USA). The measurements were conducted following the well-stirred condition (WSC) method [5, 14] which consists of measuring and analyzing the chamber S_{11} parameters from the antenna. According to its dimensions, the fundamental resonant mode frequency of the cavity is estimated to be approximately 390 MHz.

The MOF measurements were conducted for several antenna positions and orientations inside the cavity. The results were

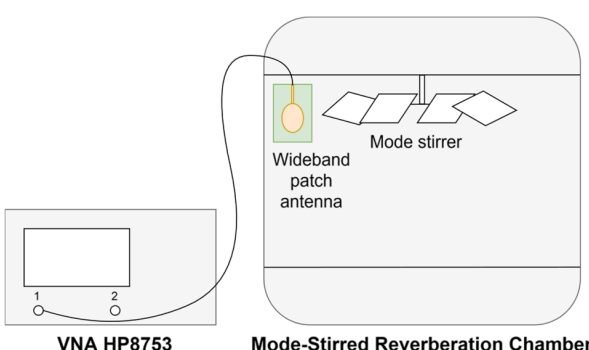


FIGURE 2. Simplified schematics of the experimental setup.

consistent, i.e., the assessed MOFs were mostly independent from the position/orientation of the antenna, similar to the results shown in [5]. For the reasons stated in Section 2.1 and because this paper focuses on the use of statistical tools, a single antenna position and orientation is considered as follows.

Let $\langle S_{11} \rangle_N$ denote the S_{11} sample mean over the N stirrer angles. $\langle S_{11} \rangle_N$ represents the maximum likelihood estimator of the S_{11} population mean. Therefore, the part of S_{11}^k due to stirred paths denoted as $S_{11,\text{sti}}^k$ may be estimated by subtracting $\langle S_{11} \rangle_N$:

$$S_{11,\text{sti}}^k = S_{11}^k - \langle S_{11} \rangle_N \quad (4)$$

The superscript k designates the k^{th} stirrer angle so that $\theta = 2\pi \frac{k}{N}$ is the stirrer position angle.

The S parameters were measured from 0.5 GHz to 6 GHz and sampled over 1601 frequency points. Statistics of $|S_{11,\text{sti}}^k|$ are supposed to be related to the statistics of the rectangular electric field magnitude next to the antenna for a given stirrer angle [16]. Hence, as explained in the introduction, $|S_{11,\text{sti}}^k|$ is expected to be asymptotically Rayleigh distributed.

The subsequent sections of this work will focus on comparing the $|S_{11,\text{sti}}^k|$ samples ECDF to the corresponding theoretical Rayleigh distribution CDF as a function of frequency. In the literature, this comparison is typically conducted using goodness-of-fit hypothesis tests. This work proposes another approach that does not involve hypothesis testing and is instead based on normalized distances.

4. USING GOF TESTS TO ASSESS THE MOF

The WSC method [5, 14] and other publications [2, 9] use hypothesis tests to assess the $|S_{11,\text{sti}}^k|_{k \in \llbracket 1; N \rrbracket}$ samples whether the $|S_{11,\text{sti}}|$ population is Rayleigh distributed. When it is the case, the MSRC is considered as effectively overmoded and operating at least partially as intended [4, 6, 14]. However, according to the central limit theorem, the transition process to a Rayleigh distribution over frequency in an MSRC is continuous and asymptotical [7, 22]. The $|S_{11,\text{sti}}|$ distribution only converges to a Rayleigh distribution. Hence, a discrepancy between the Rayleigh distribution and experimental distribution always remains. Additionally, experimental measurements carry thermal and measurement noise [23], usually contributing to the model discrepancy. Generally speaking, and in particular for the GoF tests, the statistical power of hypothesis tests increases with the sample size [21]. Therefore, any model discrepancy might be detected by a hypothesis test, provided that the sample size is large enough. In the end, the calculated MOF strongly depends on the sample size selection. This dependence is studied and discussed both experimentally and in statistical simulation in this section.

4.1. Testing Experimental Data with GoF Tests

The $|S_{11,\text{sti}}^k|_{k \in \llbracket 1; N \rrbracket}$ samples were acquired using the experimental setup shown in Figure 2. Similar to [24], the modified statistics of the AD, KS, and CvM tests from Stephens [25] are used in this study. As the critical values associated with the

modified statistics are independent of the sample size, the resulting calculations are simplified. Considering its extensive use in the literature, this section focuses on the AD test which serves here as an example.

The modified AD statistic A_m^2 is plotted in Figure 3 for different sample sizes ranging from $N = 30$ to $N = 350$. A 5th order polynomial interpolation is superimposed to the plots, similar to [5, 26]. A value of 1.341 corresponds to the critical value t_α for a significance level of 5% for the modified AD test [5]. As can be observed, when the sample size increases, the intersections of A_m^2 with t_α shift towards the high frequencies. This is expected: as the test gains in power, it becomes more capable of detecting smaller departures from the model. Consequently, both the A_m^2 statistic and MOF increase. Utilizing the modified KS and CvM tests instead of AD test is reported leading to the same conclusion.

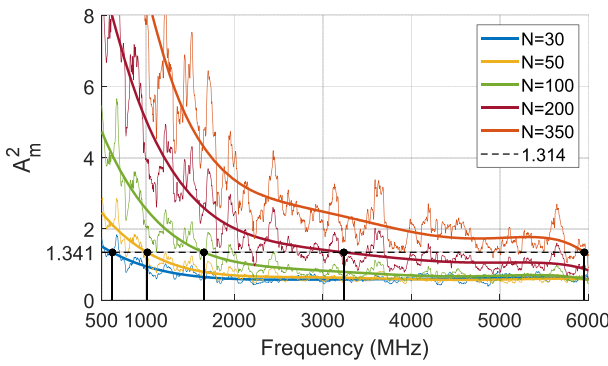


FIGURE 3. Experimental plots of the modified AD statistic A_m^2 for different sample sizes. Thick lines represent the 5th order polynomial interpolations whereas thin lines represent the moving averages over 31 points. According to the WSC method [5], the intersections with the value of 1.341 correspond to the MOF for a 5% significance level.

4.2. Running GoF Tests Statistical Simulations

In this section, a Rayleigh distributed random variable featuring additive noise is simulated. The aim of this study is to demonstrate that a distribution model discrepancy, such as additive noise, will be detected by the GoF tests, provided that the samples are large enough.

Let X be a Rayleigh distributed random variable with a distribution parameter $\sigma = 1$. To simulate the presence of additive noise, a centered normally distributed random variable Y is added to X , resulting in a random variable U given by:

$$\text{Rayleigh} \quad \text{Noise} \quad U = X + \eta Y \quad (5)$$

where η is a positive scaling coefficient. In the following, the rejection rate of a test is defined as the empirical proportion of trials that are leading to rejecting the null hypothesis, i.e., the statistic is above the critical value threshold. The rejection rate associated with the tests for a given significance level is estimated by generating a high number of observations of U .

Figure 4 shows the calculated rejection rate over 5000 trials for the AD, KS, and CvM tests as a function of the sample size for different noise coefficients η ranging from 0 to 0.3. The

FOW distance is not shown, as the critical values related to the tests using the FOW distance are usually not tabulated in the literature. As expected, the rejection rate without noise is close to 5%. However, when noise is added, the rejection rate virtually reaches 100% beyond a certain sample size. For example, with $\eta = 0.1$, the AD test only detects the additive noise for sample sizes larger than 10^3 . As predicted by the theory explained above, any departure from the ideal distribution, i.e., additive noise in this example, can be detected provided that the test has enough power. In this case, increasing the power of the test is achieved by employing larger samples.

In a mode-stirred reverberation chamber, the additive noise due to thermal fluctuations or measurement noise is not the only source of model discrepancy. The electric field rectangular component magnitude is only asymptotically Rayleigh distributed [7]. To address these issues, a new criterion based on normalized statistical distances and accounting for the subjectivity associated with the sample size selection is introduced in the next section.

5. INTRODUCING A NORMALIZED STATISTICAL DISTANCE

5.1. Definition of the Proposed Normalized Distance

In the context of determining the MOF of MSRCs, the GoF tests answer the question “Is the sample sufficiently characteristic of a Rayleigh distribution so the test overlooks the model discrepancy?” rather than the question “Is the sample drawn from a Rayleigh distribution?”. The matter here is to define what “sufficiently characteristic” means.

A relative normalized distance as a frequency function denoted as d_n is proposed, for any N , as follows:

$$d_n(f) = \frac{D_s(f) - D_{s,\infty}}{D_s(f_0) - D_{s,\infty}} \quad (6)$$

where D_s refers to any of the statistical distances listed in Table 1; $D_s(f_0)$ is the D_s statistical distance evaluated at the cavity fundamental resonance frequency f_0 ; and $D_{s,\infty}$ is the estimated asymptotical value of the distance at very high frequencies: $D_{s,\infty} = \lim_{f \rightarrow \infty} D_s(f)$. Figure 5 shows an illustration of the proposed d_n distance in (6).

The distance $D_s(f_0)$ makes no physical sense in itself. Rather, it serves as a starting point where it is known that the mode stirrer has little to no influence. The asymptotical value $D_{s,\infty}$ is to be experimentally determined. $D_{s,\infty}$ is expected to be greater than 0 because of the finite nature of the observation sets and because of model imperfections such as noise. In the case of the KS distance, the Dvoretzky-Kiefer-Wolfowitz-Massart (DKW) inequality provides an upper bound when independent observations are considered. However, the observations in this work are not truly independent, leading to an even higher expected upper bound.

The distances given in Table 1 serve as an example, and one might expand experiments with other distances. By design, d_n allows for comparing different statistical distances and also allows for limiting sample size influence. A subjective critical

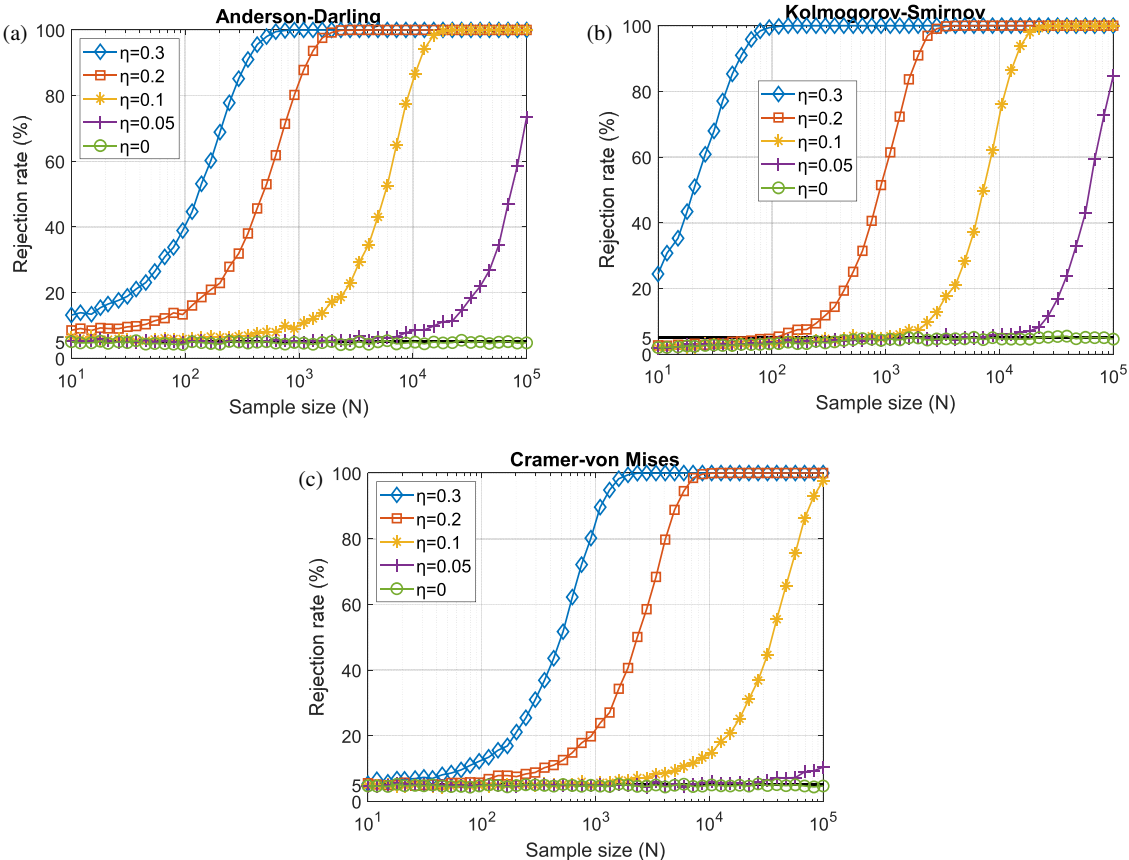


FIGURE 4. Simulation of the (a) AD, (b) KS, and (c) CvM rejection rate over 5000 trials as a function of sample size for different additive noise values and for a 5% significance level.

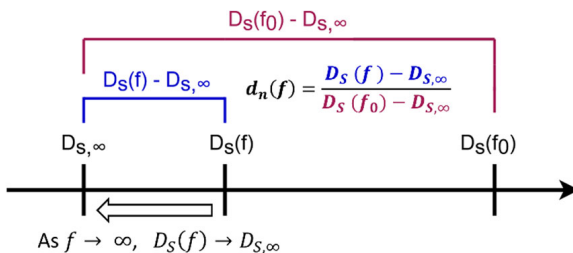


FIGURE 5. Schematic diagram illustrating the definition of the normalized distance d_n and its evolution as the frequency increases.

value T can be associated with d_n , satisfying the condition:

$$f \geq f_{\text{MOF}} \Rightarrow d_n(f) \leq T \quad (7)$$

where f_{MOF} is the assessed minimum operating frequency. For this study, an arbitrary value of $T = 0.1$ is chosen. The value of T should be chosen in accordance with the context of the conducted study and should be kept constant across all the trials. The T criterion accounts for the subjectivity introduced by the choice of both the significance level and sample size when classically using GoF tests.

5.2. Experimental Results

The following results are obtained using experimental data extracted from the reverberation chamber setup described in Sec-

tion 3. The normalized distance d_n given by (6) is plotted in Figure 6 for each of the distances listed in Table 1 with $N = 100$ sample size. It is observed that different distances present a similar behavior. The first-order Wasserstein distance converges slower than the other distances. This could be because it involves the Riemann integral, hence behaving differently from the AD and CvM distances involving the Riemann-Stieltjes integral [27].

Table 2 features the MOFs obtained by applying the proposed criterion given in Equation (7), with $T = 0.1$ and $N = 100$, to the four distances listed in Table 1. The tabulated frequencies correspond to the intersection of the polynomial curves plotted in Figure 6 with the threshold value of $T = 0.1$. Depending on the context requirements, the global assessed MOF typically is the higher or average frequency.

Figure 7 compares the minimum operating frequency f_{MOF} plotted as a function of the sample size N , for both the approaches, i.e., using the proposed normalized distances and using the GoF hypothesis tests.

The results demonstrate that the hypothesis test method diverges as the sample size increases. For small sample sizes, the determined MOF is below 500 MHz, i.e., in the vicinity of the fundamental resonance frequency of the studied electromagnetic cavity. The method introduced in this work converges and reaches a plateau value as the sample size increases. In the [30; 350] sample size range, the MOF issued from the AD hypothesis test method varies within the entire analysis band,

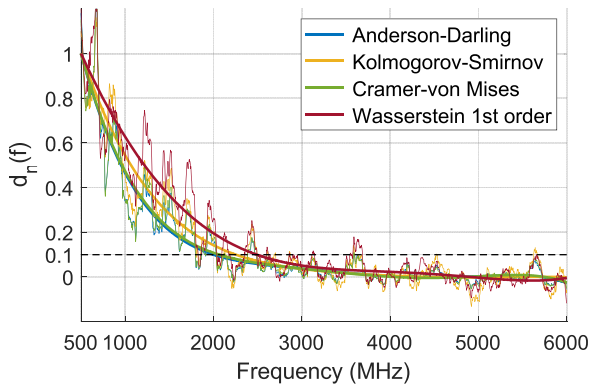


FIGURE 6. Plots of d_n for the four statistical distances listed in Table 1 and $N = 100$. Thick lines represent the 5th order polynomial interpolations whereas thin lines represent the moving averages over 31 points.

TABLE 2. Assessed lowest usable frequencies using the method described in Section 5.1 and the data plotted in Figure 6.

Distance name	f_{MOF} (GHz)
Anderson-Darling (AD)	2.00
Kolmogorov-Smirnov (KS)	2.25
Cramer-von Mises (CvM)	2.07
First-Order Wasserstein (FOW)	2.49

from 500 MHz to 6000 MHz, whereas the normalized AD distance method MOF varies from 1450 MHz to 2110 MHz and asymptotically approaches the value of 2070 MHz. Therefore, the introduced approach suggests an improvement in the reliability of the MOF estimation over the method relying on hypothesis tests.

5.3. Sample Independence Requirements

Independent samples are required for statistical tests such as AD or KS, i.e., each measurement in the sample is independent from one another. However, since the mode stirrer employed in this study consists of a rotating metallic structure, the number of actually independent samples is limited due to the stirrer periodic trajectory. In this work, the GoF tests are inevitably performed on correlated data, particularly for sample sizes above 200. A study led by Monsef et al. [18] showed that the AD test performance is degraded beyond 90% correlation. Nonetheless, sample correlation cannot entirely explain why the AD hypothesis test is failing at consistently assessing the MOF. Indeed, as shown in Figure 7, for $N = 30$ where the samples are mostly independent, the estimated MOF with the GoF method is below 500 MHz (chamber fundamental resonant frequency). In the literature, the minimum operating frequency is empirically defined around $5f_0$ or $6f_0$ [8, 15]. The MOF obtained with the proposed normalized distance method, with $T = 0.1$, corresponds to the value obtained using this empirical criterion.

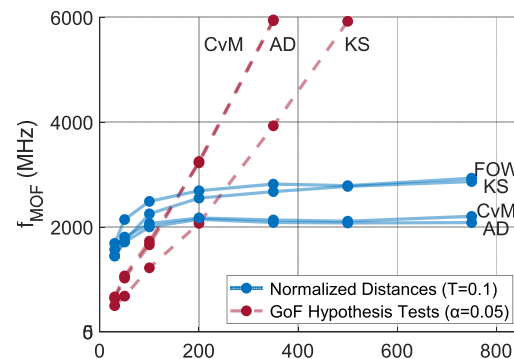


FIGURE 7. Plots of the determined MOF with both the normalized distance approach (blue curve) and the AD hypothesis test method (red curve) as function of the sample size.

6. CONCLUSION

A review has been performed on the use of goodness-of-fit hypothesis tests for assessing the minimum operating frequency of mode-stirred reverberation chambers. As evidenced, the initial intent of these tests is the detection of statistically significant results instead of validating the null hypothesis associated with the population distribution. As a consequence of this logical inversion, the estimated MOFs using these tests are drastically impacted by the sample size selection, which is directly associated with the test statistical power of the tests.

To overcome the uncertainty associated with the subjectivity on the sample size selection, a new approach was introduced based on normalized statistical distances. By accepting a subjective criterion, denoted as T on the normalized distances, the sample size influence on the MOF estimation was limited. Moreover, the suggested normalized distance allows for MOF consistency probing by comparing different statistical distances. As shown previously, the proposed approach in this study allows for more consistent results. When normalized distances are used, the effect of sample size selection is drastically reduced compared to when GoF hypothesis tests are used.

The method proposed in this paper offers a new approach to assess the MOF and could be relevant in the straightforward characterization processes of the mode-stirred reverberation chambers.

ACKNOWLEDGEMENT

This work is supported by institutional grants from the French National Research Agency under the Investments for the future program with the reference ANR-18-EURE-0017 TACTIC and from the French Agency for Food, Environmental and Occupational Health & Safety grants numbers 5G-S-CARE — 2023_RF_010 and 5G-HumBO-2021_2 RF_24.

REFERENCES

- [1] Rajamani, V., C. Bunting, and G. Freyer, "Why consider EMC testing in a reverberation chamber," in *2008 10th International Conference on Electromagnetic Interference & Compatibility*,

303–308, Bangalore, India, Nov. 2008.

[2] Orlacchio, R., G. Andrieu, A. Joushomme, L. Patrignoni, A. Hurtier, F. P. D. Gannes, I. Lagroye, Y. Percherancier, D. Arnaud-Cormos, and P. Leveque, “A novel reverberation chamber for in vitro bioelectromagnetic experiments at 3.5 GHz,” *IEEE Transactions on Electromagnetic Compatibility*, Vol. 65, No. 1, 39–50, Feb. 2023.

[3] Paolanti, M., R. Pollini, E. Frontoni, A. Mancini, R. D. Leo, P. Zingaretti, and B. Bisceglia, “Exposure protocol setup for agro food treatment. Method and system for developing an application for heating in reverberation chamber,” in *2015 IEEE 15th Mediterranean Microwave Symposium (MMS)*, 1–4, Lecce, Italy, Nov. 2015.

[4] Chen, X., “Model selection for investigation of the field distribution in a reverberation chamber,” *Progress In Electromagnetics Research M*, Vol. 28, 169–183, 2013.

[5] Andrieu, G., N. Ticaud, F. Lescoat, and L. Trougnou, “Fast and accurate assessment of the “well stirred condition” of a reverberation chamber from S_{11} measurements,” *IEEE Transactions on Electromagnetic Compatibility*, Vol. 61, No. 4, 974–982, Aug. 2019.

[6] Fall, A. K., P. Besnier, C. Lemoine, M. Zhadobov, and R. Sauleau, “Design and experimental validation of a mode-stirred reverberation chamber at millimeter waves,” *IEEE Transactions on Electromagnetic Compatibility*, Vol. 57, No. 1, 12–21, Feb. 2015.

[7] Lemoine, C., P. Besnier, and M. Drissi, “Investigation of reverberation chamber measurements through high-power goodness-of-fit tests,” *IEEE Transactions on Electromagnetic Compatibility*, Vol. 49, No. 4, 745–755, Nov. 2007.

[8] Primiani, V. M. and F. Moglie, “Numerical simulation of reverberation chamber parameters affecting the received power statistics,” *IEEE Transactions on Electromagnetic Compatibility*, Vol. 54, No. 3, 522–532, Jun. 2012.

[9] Xu, Q., L. Xing, Y. Zhao, T. Jia, and Y. Huang, “A source stirred reverberation chamber using a robotic arm,” *IEEE Transactions on Electromagnetic Compatibility*, Vol. 62, No. 2, 631–634, Apr. 2020.

[10] He, Y. and A. C. Marvin, “Aspects of field statistics inside nested frequency-stirred reverberation chambers,” in *2009 IEEE International Symposium on Electromagnetic Compatibility*, 171–176, Austin, TX, USA, Aug. 2009.

[11] Monsef, F. and A. Cozza, “Goodness-of-fit tests in radiated susceptibility tests,” in *2012 ESA Workshop on Aerospace EMC*, 1–5, Venice, Italy, 2012.

[12] Markatou, M., D. Karlis, and Y. Ding, “Distance-based statistical inference,” *Annual Review of Statistics and Its Application*, Vol. 8, No. 1, 301–327, Mar. 2021.

[13] Hill, D. A., “Plane wave integral representation for fields in reverberation chambers,” *IEEE Transactions on Electromagnetic Compatibility*, Vol. 40, No. 3, 209–217, Aug. 1998.

[14] Andrieu, G., *Electromagnetic Reverberation Chambers: Recent Advances and Innovative Applications*, Guillaume Andrieu, SciTech Publishing, The Institution of Engineering and Technology, 2021.

[15] Démoulin, B. and P. Besnier, *Les Chambres Réverbérantes en Electromagnétisme*, Hermès Lavoisier, 2010.

[16] Lemoine, C., E. Amador, and P. Besnier, “On the K-factor estimation for rician channel simulated in reverberation chamber,” *IEEE Transactions on Antennas and Propagation*, Vol. 59, No. 3, 1003–1012, Mar. 2011.

[17] Hill, D. A., “Boundary fields in reverberation chambers,” *IEEE Transactions on Electromagnetic Compatibility*, Vol. 47, No. 2, 281–290, May 2005.

[18] Monsef, F., R. Serra, and A. Cozza, “Goodness-of-fit tests in reverberation chambers: Is sample independence necessary?” *IEEE Transactions on Electromagnetic Compatibility*, Vol. 57, No. 6, 1748–1751, Dec. 2015.

[19] Laio, F., “Cramer-von Mises and Anderson-Darling goodness of fit tests for extreme value distributions with unknown parameters,” *Water Resources Research*, Vol. 40, No. 9, 2004.

[20] Dedecker, J. and F. Merlevède, “Behavior of the Wasserstein distance between the empirical and the marginal distributions of stationary α -dependent sequences,” *Bernoulli*, Vol. 23, No. 3, 2083–2127, Aug. 2017.

[21] Sachs, L., *Applied Statistics*, Springer Series in Statistics, Springer, New York, NY, 1984.

[22] Monsef, F. and A. Cozza, “A possible minimum relevance requirement for a statistical approach in a reverberation chamber,” *IEEE Transactions on Electromagnetic Compatibility*, Vol. 57, No. 6, 1728–1731, Dec. 2015.

[23] Nyquist, H., “Thermal agitation of electric charge in conductors,” *Physical Review*, Vol. 32, No. 1, 110, Jul. 1928.

[24] Zhai, S., X. Zhou, P. Hu, Y. Chen, D. Chen, Z. Zhou, and M. Sheng, “Alternative method for the determination of the ideal electromagnetic reverberant frequency with frequency stirring technique,” *IEICE Electronics Express*, Vol. 18, No. 6, 20210069, 2021.

[25] Stephens, M. A., “EDF statistics for goodness of fit and some comparisons,” *Journal of the American Statistical Association*, Vol. 69, No. 347, 730–737, 1974.

[26] Yousaf, J., M. Ghazal, H. Lee, M. Faisal, J. G. Yang, and W. Nah, “Efficient assessment of well-stirred operation of reverberation chamber using coupling transfer gain functions,” *Journal of Electromagnetic Waves and Applications*, Vol. 35, No. 3, 315–335, Feb. 2021.

[27] Anevski, D., “Riemann-stieltjes integrals,” Lecture Notes, Lund University, Sweden, 2012.